Single-Anchor Indoor Localization Using a Switched-Beam Antenna

Gianni Giorgetti, Alessandro Cidronali, *Member, IEEE,*
Sandeep K. S. Gupta, *Senior Member, IEEE,* and Gianfranco Manes, *Senior Member, IEEE*

***Abstract*—We propose an RF-based localization system that works using a single anchor node. The anchor is equipped with a switched-beam directional antenna that is installed on the ceiling of a room and collects signal strength information sufficient for absolute 2D target positioning. Indoor measurements are used to show satisfactory localization results with range-free (proximity), range-based and fingerprinting schemes.**

***Index Terms*—Directional antenna, switched-beam, localization, proximity, DOA, fingerprinting.**

I. Introduction

SMART antennas have been used to implement localization systems based on *Angle of Arrival* (AOA) estimation [1], [5]. This approach improves over *Received Signal Strength* (RSS) ranging schemes for two reasons. First, AOA estimates can be obtained without assumptions on the propagation model that relates the RSS to the distance. Second, AOA-based localization requires only two anchors, while at least three reference nodes are needed when using distance estimates.

We take the directional approach one step further by proposing an indoor localization system with a single anchor node. The node, which serves as a Base Station (BS), is equipped with a switched-beam antenna (Fig. 1) that is installed on the ceiling of any large indoor space, in a position unobtrusive to the users. Thanks to the 3D arrangement of the antenna faces, the system can locate a target by estimating both the azimuth θ_t and elevation ϕ_t AOA of the incoming messages.

Our solution targets applications in large rooms or indoor open spaces where installing a network of anchors is not desirable or feasible. Possible application scenarios include low-cost deployments and ad-hoc applications (e.g. emergency response). To accommodate for different sets of requirements in terms of accuracy and costs, we propose three localization solutions. We describe a *range-free* (proximity), a *range-based* and a *fingerprinting* localization approach. The proposed schemes, which are evaluated using RSS traces from a real deployment, show that satisfactory localization results are possible using a single anchor node.

II. Antenna

The antenna mounted on the BS was designed with the goal to implement a compact, low-cost system with a steerable beam capable of selectively illuminating the space underneath the BS and collecting information useful for target localization.

Manuscript received September 30, 2008. The associate editor coordinating the review of this letter and approving it for publication was H.-H. Chen.

G. Giorgetti and S. K. S. Gupta are with the IMPACT Lab (impact.asu.edu), Arizona State University, Tempe, AZ 85287, USA (e-mail: {gianni.giorgetti, sandeep.gupta}@asu.edu).

A. Cidronali and G. Manes are with the Department of Electronics and Telecommunications of the University of Florence, Italy (e-mail: {alessandro.cidronali, gianfranco.manes}@unifi.it).

Digital Object Identifier 10.1109/LCOMM.2009.081584

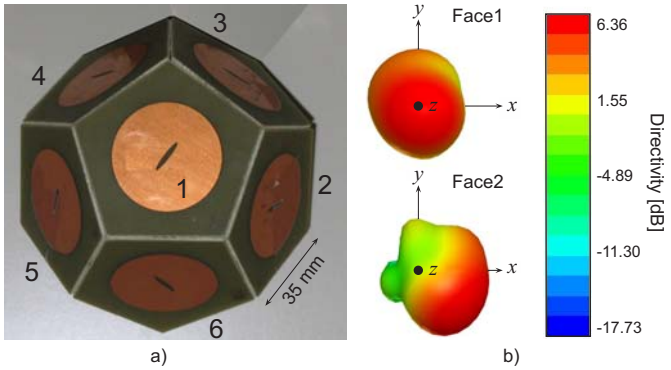

Fig. 1. a) Bottom-up view of the switched-beam directional antenna. b) Simulated radiation patterns when faces 1 and 2 are active.

The proposed solution is an incoherent array of six adjacent radiating elements, assembled to form a semi dodecahedron (see Fig. 1a). Each element is implemented in microstrip antenna technology on a pentagonal plastic substrate and fed by a coaxial probe. The operating frequency is 2.45 GHz with a bandwidth compatible with IEEE 802.11 and IEEE 802.15.x devices such as WLAN, Bluetooth and ZigBee transceivers. Given the intended use in indoor applications, we adopted a circular polarization design that has proven useful in mitigating multipath effects in reflective environments [2].

A single-pole six-through RF switch is used to multiplex each radiating element. Under control of the BS, the switch connects one of the six radiators to the transceiver. The inactive faces, which are terminated on matched loads, behave as dummy loads, without significantly perturbing the radiation pattern of the active patch. Figure 1b shows two of the six radiation patterns simulated using the Ansoft HFSS software[1]. The directivity is typical to that of a microstrip antenna, with the main lobe pointing in the direction perpendicular to the active face.

III. Localization

We have implemented a *proof-of-concept* application where the antenna is used to estimate the position (x_t, y_t) of a mobile target in a large classroom containing rows of desks and chairs. The antenna was placed approximately in the center of the room, two meters above the desks, and with the face 1 pointing toward the floor. We collected RSS traces on a 6×4 grid (see Fig. 2) by exchanging bursts of 100 messages between the target and each of the six antenna faces. We have used the measured data to evaluate the performance of three different localization algorithms described in the following sections.

[1]http://www.ansoft.com/products/hf/hfss/

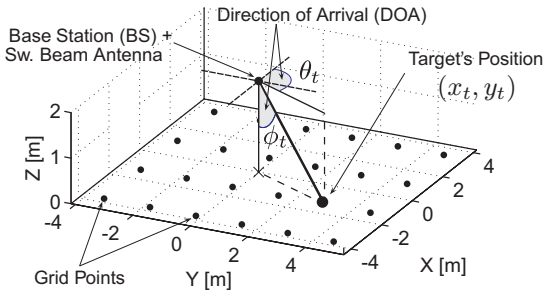

Fig. 2. Deployment area and 6×4 measurement grid. The grid covers an area measuring $7.2\,\text{m} \times 8\,\text{m}$. Both the BS and the target use a TI CC2420 transceivers set to transmit at -15 dBm.

A. Principle of operations

Let the pair of angles (ϕ_t, θ_t) define the *Direction of Arrival* (DOA) of the target's messages. According to the Friis' equation, the received power depends on the target's distance and antenna gains $G_i(\phi_t, \theta_t)$ obtained from the radiation patterns in Fig. 1b. Given the small antenna dimensions, all the faces are at about the same distance from the target; therefore, the differences in received power (in dB) between two faces i and j will only depend on their gains:

$$P_i - P_j = G_i(\phi_t, \theta_t) - G_j(\phi_t, \theta_t). \tag{1}$$

Note that, with fixed antenna position and assuming target's movements in the plane $z = 0$, there is a one-to-one correspondence between the DOA (ϕ_t, θ_t) and the target's position (x_t, y_t). We let m be the bijective function that describes the mapping:

$$m : (x_t, y_t) \longrightarrow (\phi_t, \theta_t). \tag{2}$$

In the following sections we will show how the above relation can be exploited to estimate the target's position.

B. Range-Free Localization (Proximity)

The first approach we evaluate is a range-free scheme that provides coarse-grained localization. This solution bears resemblance to a simple proximity-based scheme, but instead of relying on a set of anchor nodes, it only uses measurements from the switched-beam antenna.

To implement our solution, we use the radiation patterns and (2) to partition the deployment area in a set of non-overlapping regions $S_1, \ldots, S_6$. These regions are computed by comparing the gains $G_i(m(x, y))$ seen in different locations of the deployment area (see top row of Fig. 3):

$$S_i = \{(x, y) : G_i(m(x, y)) > G_j(m(x, y)), \forall i \neq j\}. \tag{3}$$

Each area S_i contains the locations that are best illuminated by face i. In an ideal environment, face i would receive the strongest signal (compared to the other faces) for any message sent from locations $(x_t, y_t) \in S_i$. Assuming a more realistic propagation model, the constraints on the RSS can only be formulated in a statistical sense. For example, when the signal is described by the widely adopted *log-normal shadowing model* [6], the average RSS (in dB) follows a normal distribution. In this case, each area S_i contains the locations where the statical expectation for the power on face i is larger than the expected values on the other faces.

Based on the previous observations, at runtime we assign the target's position to the area S_i that corresponds to the face measuring the strongest (average) signal:

$$(\hat{x}_t, \hat{y}_t) \in S_{i_{\max}}, \quad \text{with} \quad i_{\max} = \arg \max_{i \in [1,6]} \{\bar{z}_i\}, \tag{4}$$

where $\bar{z}_i$ is the mean of the RSS values $\mathbf{z_i} = \{z_1^{(i)}, z_2^{(i)}, \ldots\}$ collected by each face i. Note that the computational requirements of this approach are minimal because the regions S_i are computed off-line and only depend on the antenna position and its radiation patterns. In particular, by varying the antenna's height it is possible to adjust the size of the areas S_i and control how the deployment area is partitioned.

We used the measured RSS data (see bottom row of Fig. 3) to evaluate the result of the assignment (4). Figure 4a shows the deployment area partitioned according to the areas S_i and the classification results on the 6×4 grid points. To each point we assigned an error equal to the distance between its position and the center of the area $S_{i_{\max}}$ computed using (4). The average error is equal to $2.34\,\text{m}$. Although the resolution is limited to the six areas S_i, the simplicity of this approach is attractive to applications that can tolerate approximate positions. The results could be further improved by computing the regions S_i using more sophisticated models, such as the ray tracing approach adopted in [7].

C. Range-Based Localization (DOA Estimation)

The second solution implemented uses the measured RSS values to estimate the DOA $(\hat{\phi}_t, \hat{\theta}_t)$ of the incoming pack-

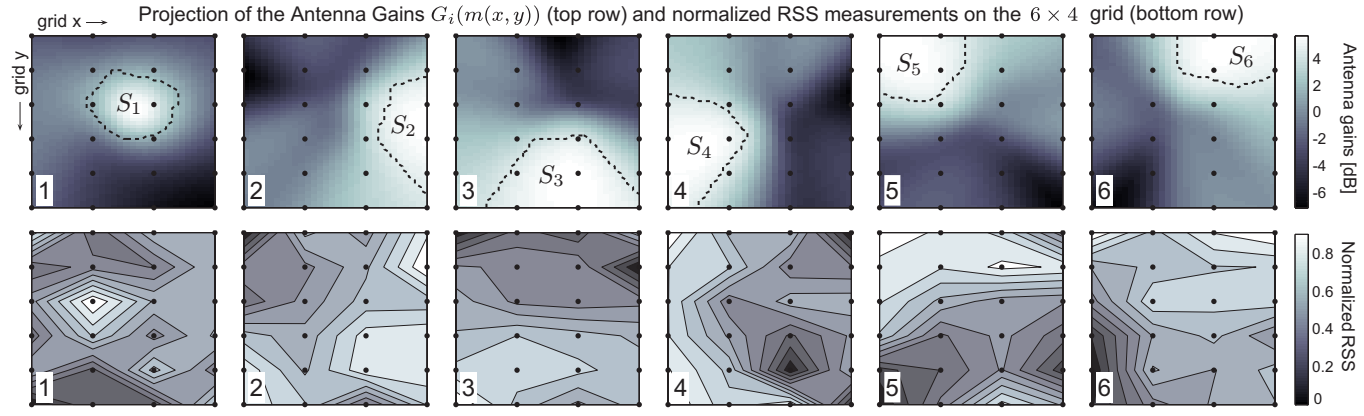

Fig. 3. **Top**: antenna gains of faces 1 to 6 at different locations of the deployment area. **Bottom**: measured RSS values from the six antenna faces on the 6×4 grid. To facilitate comparison with the gain values, the RSS values are centered on their mean and normalized in the range $[0, 1]$.

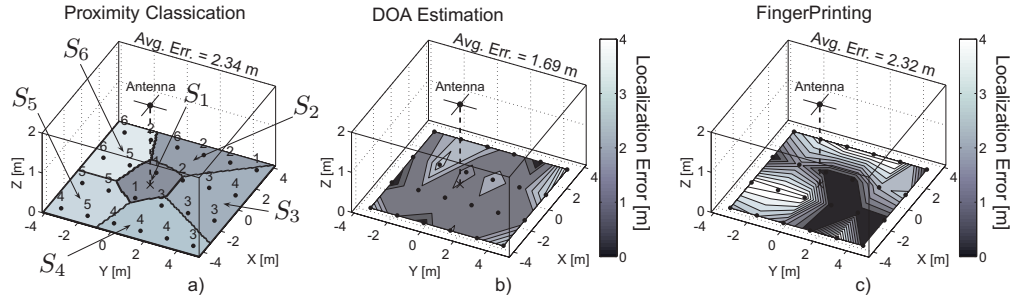

Fig. 4. Localization results using a) Proximity-based classification, b) DOA Estimation, and c) Fingerprinting.

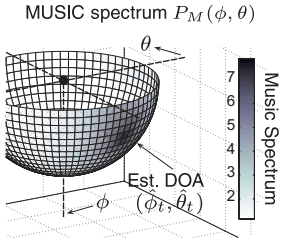

Fig. 5. MUSIC spectrum $P_M(\phi,\theta)$ represented in spherical coordinate system centered on the antenna.

ets. Our implementation uses the popular *Multiple Signal Classification* (MUSIC) approach [3], which applies spectral decomposition to the covariance matrix of the power readings on each face. The MUSIC algorithm produces a "spectrum" $P_M(\phi,\theta)$ that exhibits peaks for angles (ϕ,θ) close to the true DOA. An example of such spectrum is shown in Fig. 5. After computing $P_M(\phi,\theta)$, we estimate the DOA by selecting the angles that yield the maximum spectrum value; then we apply the inverse of (2) to resolve the target position:

$$(\hat{x}_t, \hat{y}_t) = m^{-1}(\hat{\phi}_t, \hat{\theta}_t), \tag{5}$$

where $(\hat{\phi}_t, \hat{\theta}_t) = \arg\max_{(\phi,\theta)} P_M(\phi,\theta)$.

Compared to the previous case, this method is computationally more expensive, but it allows for fine-grained localization. Figure 4b shows the localization error using the same set of RSS measurements of the previous case. We found an average localization error equal to $1.69\,\mathrm{m}$.

This approach extends previous solutions exploiting beacons with directional antennas located on the target's plane [1], [5]. When DOA estimation is limited to the azimuth angle θ_t, single-anchor localization is not possible unless combined with distance estimates obtained from RSS measurements. In our case, since both the azimuth θ_t and elevation angles ϕ_t are estimated, target positions in the $z = 0$ plane can be resolved without need of additional information.

D. Fingerprinting

The last solution tested is a fingerprinting scheme that estimates the target's position by comparing the RSS on the six antenna's faces against a database of previously measured values. This approach offers a low-computation solution that is oblivious of the RF propagation model and the antenna gains. On the downside, it requires a site survey to collect RSS signatures at several locations of the deployment area.

In our implementation we created the database by using the average RSS values $[\bar{z}_1, \ldots, \bar{z}_6]$ collected on the 6×4 grid (see Fig. 3); we evaluated the localization error using a second set of similar measurements. Each location was estimated by first computing the Euclidean distance between the actual RSS values and the stored measurements, and then applying a *K-Nearest Neighbor* (KNN) regression algorithm [4]. The better results were achieved by setting $K = 1$, which yielded an average localization error equal to $2.32\,\mathrm{m}$ (see Fig. 4b).

We suspect that the large error on some grid points was caused by the different type of antenna mounted on the target device in the second round of measurements.

IV. Conclusions

The proximity and range-based approaches discussed in Sec. III-B and III-C are based on the DOA of the target's messages. These schemes are suited for large rooms or indoor open spaces where *Line Of Sight* (LOS) communication with the BS station can be ensured. Outdoor localization can be also supported by placing the BS at a sufficient height.

When LOS communication is possible, the results of our experiments show that single-anchor 2D localization is feasible using a low-cost system that requires zero-configuration. The reported results were obtained with an initial antenna prototype optimized for size and using simulated radiation patterns. We believe the error could be further reduced by using antenna faces with larger ground planes and radiation patterns measured in an anechoic chamber.

We expect larger errors in cluttered environments and for non LOS communication. For such applications, the fingerprinting approach discussed in Sec. III-D represents a viable solution. The results are comparable to other fingerprinting solutions described in literature [4], and the use of a single anchor can alleviate the deployment costs when an infrastructure of anchors is not already available.

Acknowledgments

We thank S. Maddio and S. Maurri for help in designing and building the antenna prototype; F. Zucchelli and N. Corsi for help with measurements; the anonymous reviewers for their helpful comments; and NSF for support.

References

[1] J. N. Ash and L. Potter, "Sensor network localization via received signal strength measurements with directional antennas," in *Proc. Allerton Conf. on Communication, Control, and Computing*, 1861–1870, 2004.

[2] A. Kajiwara, "Line-of-sight indoor radio communication using circular polarized waves," *IEEE Trans. Veh. Technol.*, vol. 44, no. 3, pp. 487–493, 1995.

[3] H. Krim and M. Viberg, "Two decades of array signal processing research: the parametric approach," *IEEE Signal Proc. Mag.*, vol. 13, no. 4, pp. 67–94, 1996.

[4] H. Liu *et al.*, "Survey of wireless indoor positioning techniques and systems," *IEEE Trans. Systems Man and Cybernetics*, vol. 37, no. 6, pp. 1067–1080, 2007.

[5] D. Niculescu and B. Nath, "VOR base stations for indoor 802.11 positioning," in *Proc. MobiCom'04*, pp. 58–69, 2004.

[6] T. S. Rappaport, *Wireless Communications: Principles and Practice*. Prentice Hall, Inc., 1996.

[7] G. Zàruba *et al.*, "Indoor location tracking using RSSI readings from a single Wi-Fi access point," *Wireless Networks*, vol. 13, no. 2, pp. 221–235, 2007.